Coordinated Voltage Control in Active Distribution Network with On-load Tap Changer and Solar PV System Systems

Praveen Prakash Singh
Department of Energy Technology, 2019

Master Project

Department of Energy technology
Aalborg University
Pontoppidanstræde 111, 9220 Aalborg
http://www.et.aau.dk

AALBORG UNIVERSITY
STUDENT REPORT

Title:
Coordinated Voltage Control in Active Distribution Network with On-load Tap Changer and Solar PV System

Theme:
Master's thesis

Project Period:
Spring semester 2019

Project Group:
EPSH

Participant(s):
Praveen Prakash Singh

Supervisor(s):
Jayakrishnan Radhakrishna Pillai
Sanjay Chaudhary

Copies: 1

Page Numbers: 40

Date of Completion:
October 31, 2019

Abstract:

Decreasing cost and favorable policies have resulted in increased penetration of solar PV within active distribution network. As the penetration of PV system is likely to increase in future, utilizing the reactive power capability to mitigate overvoltage is analyzed. In recent years, droop control of inverter based distributed energy resources has emerged an as essential tool which will be investigated in this work. The participation of PV system in voltage regulation and its coordination with existing controllers such as OLTC is paramount to regulate the voltage within the specified limits. Developing control strategies which can be coordinated with the existing control in a distributed manner is proposed in this work.

Contents

Preface

This project is about voltage control in active distribution network in the presence of Solar PV system. A coordinated control approach is required to operate the active distribution network within permisisble voltage range.

I would like thank my Associate Professor Jayakrishnan Radhakrishna Pillai for giving me the chance to make a research in Voltage control using OLTC and Q-V droop control which is very interesting topic and for their extensive support during this semester. I would like also thanks Associate Professor Sanjay Chaudhary for his advises. Finally, I would like to thank my father and brothers for supporting me and understand my stress this period.

Aalborg University, October 31, 2019

Praveen Parakash Singh
<ppsi17@student.aau.dk>

Chapter 1

Introduction

A brief review of the relevant topics in transmuting energy sector is presented in this chapter. The general motivation and background manifest the ambitions of escalating the integration of distributed energy resources (DER's) in the active distribution network, and the key issues are addressed. Consequently, the problem statement bounded by a few limitations is described and the methodology used to solve the problems are presented in further sections. Finally, the outline of the thesis is summarized and contextualized.

1.1 General Background and Motivation

Global renewable energy deployment has been on the forefront in Europe over two decades to curtail the rise in temperature "well below 2° C" concerning pre-industrial levels. The fastest growing technology in renewable power generation until 2017 is solar PV (98 GW) than other renewable peers such as large hydro (19 GW) and wind (52 GW) [1]. The cost reduction of critical technologies such as PV, wind and other renewable sources accompanied by improvised end-user technology, the EU is currently on course for accomplishing the objective of 20% renewable share by 2020 and attain global leadership by 2030 with a share of 27% which can be increased to 34% taking energy efficiency into account (see Fig. 1.1) [2].

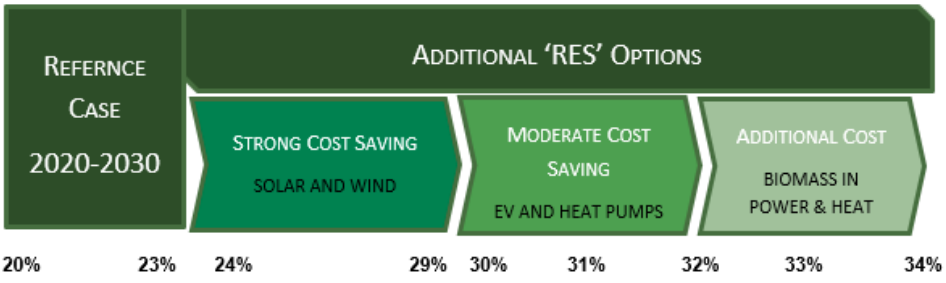

Figure 1.1: Renewable energy options for 2030 target [2]

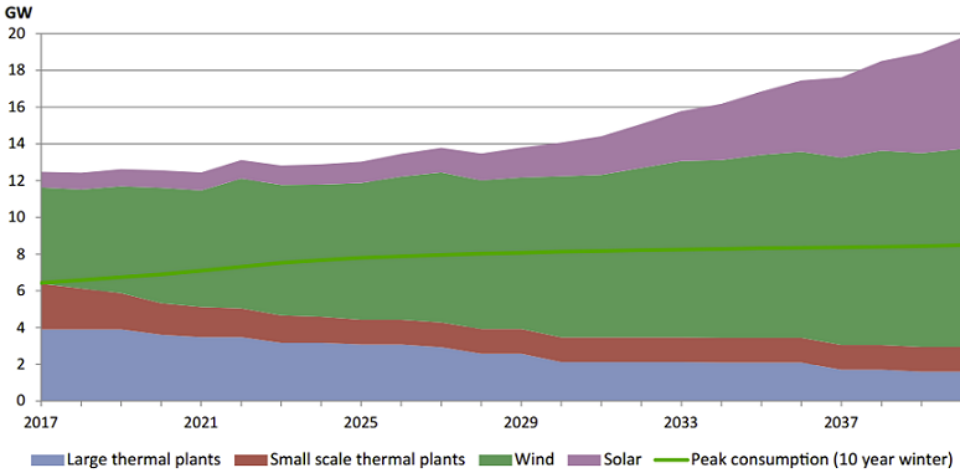

Figure 1.2: Expected future trend of Danish installed generation [3]

The Danish power system constitutes the highest share of variable renewable energy in which wind power has a share of 44% while PV production contribution is only 2% of the total Danish electricity consumption in 2017 (see Fig. 1.2) [3]. It can also be inferred that the electricity demand is lower than the generation which might increase in the future increasing the burden on the grid which may adversely affect the performance and operation of the grid. Escalating renewable power production have resulted in growth of the distributed energy resources (DER) in the distribution system. The intermittent nature of variable renewable energy resources such as solar and wind power production along with the arbitrarily changing load demand necessitates the increase in flexibility of the grid. The mismatch between the generation and demand i.e. the residual load management is a critical aspect for determining the power system flexibility needs which can be achieved by increasing interconnections, power-to-X, demand side response and storage. Flexible generation may also be used in case of high demand. [4].

Voltage control issue in presence of DER in the distribution grid has been a subject of interest for many years and various approaches have been suggested by many researchers. A summary of steady-state and dynamic effect of solar photovoltaic penetration in the distribution network given in [5], addressed issues such as malfunctioning of voltage regulating devices and/or OLTC transformer, overloading of distribution feeder, voltage flicker and unbalance among others. In [6], investigation of distribution system due to reversal of power flow resulting in notable adjustment in power factor may alter the performance of transformer in regulating the voltage of the system. The technical solutions considering voltage and thermal limits to enhance the distribution system operator (DSO) access to flexibility as proposed in [7] are advanced control of HV/MV transformer, DSO storage, on-load tap changer for MV/LV transformers, network reinforcement and reconfiguration to enhance PV hosting capacity. In [6], the impact on voltage regulation using OLTC transformers with and without LDC in medium voltage feeders with distributed generation is presented. General Electrics (GE) in [8] illustrated the control of power electronics inside smart inverter for voltage support investigating the constant power factor mode and Volt/-VAR control function. A coordinated control of battery energy storage system (BESS) with

OLTC in LV networks is reported in [9] to reduce the reverse power flow and operation of tap changer minimizing the resistive losses. In [10], the determination of BESS capacity based on load levelling and voltage control is proposed for a distribution system with a single solar PV plant located at the remote terminal. Based on the control zones determined for OLTC and DG, an approach for voltage regulation of the feeder with minimum coordination is presented in [11].

Accrediting the above mentioned modifications, the design principle of the power distribution grids based on "centralized generation follows the demand" has become invalid with increase in DER's. Integration of solar PV systems and battery energy storage system (BESS) in the grid have increased the responsibilities on the DSO's in managing the local network voltage and feeder congestion. To encounter the technical challenges at national level various recommendations as proposed in are suggested. To encounter the insufficiency in accessing the PV inverter capabilities such as curtailment of power feed at PCC, active power control P(U) and reactive power control Q(U) or Q(P) among many others. Further it is suggested that DSO access to storage system directly connect at MV/LV network could avoid upgrading transformers and controlling current in feeders

1.2 Problem Statement

The medium voltage distribution networks which conjoins the transmission system and the low voltage distribution system is paramount in delivering the power. Hence, it is necessary to investigate the performance of MV network in presence o PV and storage system.
Challenges in operation and control of an active medium voltage distribution network have been investigated in this thesis with local node voltage rise at the point of DER connection as the main issue. As the presence of solar photo-voltaic system with battery energy storage are increasing, the necessity of deigning a suitable hierarchical control structure incorporating traditional controllers such as OLTC to mitigate the issue of voltage rise has been proposed considering the constraints such as transformer loading and feeder ampacity violation .

1.3 Objectives

Addressing the problem statement, the realization of the main aim involves accomplishment of following objectives summarized as:

- Steady-state analysis of medium voltage distribution network and the effect of solar PV on the grid voltage. Analyzing the behaviour of OLTC and PV droop control on MV grid In presence of PV system.
- Design and implementation of suitable coordinated hierarchical control algorithm and investigation of grids dynamic performance.
- Comparison of coordinated and uncoordinated control of the solar PV system and OLTC along with performance evaluation of the grid.

1.4 Limitation

There are several limitation which are assumed which are enlisted below

- The network is assumed to be balanced.
- The solar PV system is considered as static generator.
- The transient and dynamic behaviour of OLTC and PV control has not been considered.
-

Chapter 2

State of Art

In this chapter, a literature review of the relevant topics related to the voltage drop along the feeder and its compensation technique using on-load tap changer along with line drop compensation technique is discussed. An overview of solar PV and battery energy storage system is presented along with the control techniques used for voltage regulation. A review of the grid codes involved in this project are also analyzed.

2.1 Overview of Distribution system

The CIGRE Task Force (TF) C6.04.02 in [12] has developed a hierarchical four level structure (see figure 2.1) which categorises the resource side benchmark dedicated to the DER's connected to electrical nodes and the network branches i.e. transmission and distribution system. The later can be further distinguished based on the voltage levels and network topology. The most common toplogies in distribution system are radial,loop and meshed.

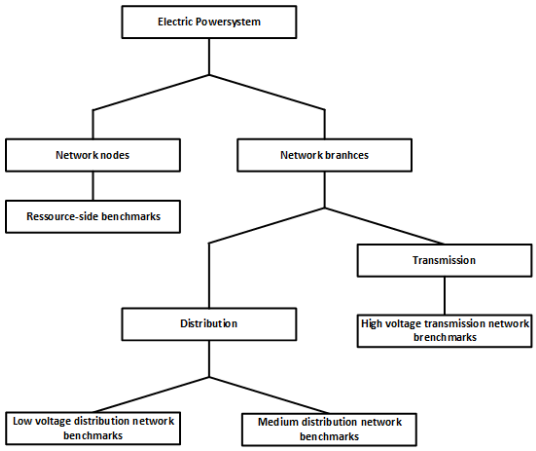

Figure 2.1: Hierarchical structure of benchmarks

The radial system are simple and cost effective in which current flows is unidirectional.

In case of loop system two radially operating feeders are connected at the remote terminal to form a ring like structure and the flow of current is bidirectional. The meshed system constitutes a large interconnection of feeders having high complexity and reliability [13].

The Distribution feeder is generally expressed as lumped π-model [14][15] as shown in figure x which constitutes series resistance (R_L) and inductance (X_L) and the shunt component represents the susceptance (B) of the line. The voltage and current at both (sending and receiving) end can be related by :

$$\begin{vmatrix} U_s \\ I_s \end{vmatrix} = \begin{vmatrix} 1 + \frac{1}{2ZYl^2} & Zl \\ Yl(1 + \frac{ZYl^2}{4}) & 1 + \frac{1}{2ZYl^2} \end{vmatrix} \begin{vmatrix} V_r \\ -I_r \end{vmatrix} \tag{2.1}$$

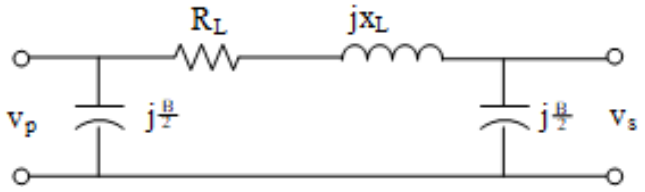

Figure 2.2: Distribution feeder π-model

Expressing the impedance of line as admittance ($Y = Z^{-1}$), the power flow equation for between the sending and receiving end can be given as [16]:

$$S_{PSL} = V_P^2(G_L + jB_L + Bsh/2) - V_P V_S(G_L + jB_L)e^{-}j(\theta_P - \theta_S) \tag{2.2}$$

This non-linear power flow equation is solved using iterative method such as Gauss-Seidel and Newtwon-Rapshon which will be considered in the next chapter.

2.2 Impact of DER on Voltage Drop in Distribution System

The voltage drop caused due to the flow of current can be analyzed using a simple single line diagram (see figure 2.3). Let us consider a simple feeder having impedance $Z(R + jX)$ through which power flows from sending end (U_S) to receiving end voltage (U_R) to supply the load $(P_L + jQ_L)$.The complex line current can be expressed as the ratio of receiving end apparent power and voltage [17]:

$$I = \frac{S_R^*}{U_R^*} = \frac{P_R - jQ_R}{U_R^*} \tag{2.3}$$

where $P_R + jQ_R = (P_L - P_G) + j(Q_L - Q_G)$. Initially it is assumed that no contribution is made from the PV. Also, the voltage drop along the distribution feeder i.e. difference between the sending and receiving end voltage can be given as [18]:

$$\Delta V = \mid U_S \mid - \mid U_R \mid = I.Z \tag{2.4}$$

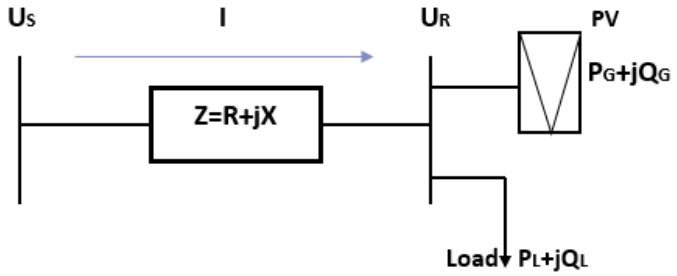

Figure 2.3: Single line diagram of a feeder connected with PV and load

The phasor diagram (see figure 2.4) assumes that the current lags the voltage (i.e.X>R) by an angle ϕ and no contribution is made by the PV. The shunt capacitance is also assumed to be negligible. The current vector can be resolved into active and reactive components which can be substituted in eq.((2.2) to give an approximated voltage drop as [18], [19]:

$$\Delta U = IRcos\phi + IXsin\phi \tag{2.5}$$

Considering O as the center, if a circle is drawn of radius U_S, the difference between the estimated and actual voltage drop can be calculated (see figure 2.4). This error can be expressed as [19]:

$$error = U_S - \sqrt{U_S^2 - (IXcos\phi - IRsin\phi)^2} \tag{2.6}$$

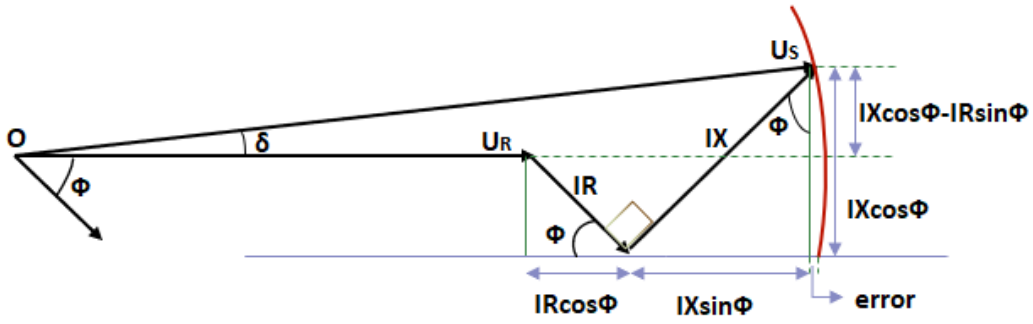

Figure 2.4: Phasor diagram of a feeder connected with PV and load

The actual voltage drop along a feeder can be obtained by adding equations (2.5) and (2.6) (see eq. (2.1)). It can be inferred that the voltage drop depends on the R/X ratio, load current and phase angle between load current and receiving end voltage. When PV

is taken into account, the voltage drop change in current which can be expressed as:

$$I = \frac{(P_R - P_{PV}) - j(Q_R - Q_{PV})}{U_R^*} \tag{2.7}$$

where P_{PV} and Q_{PV} is real and reactive power generated by the PV. The sign convention of reactive power associated to the converter may change as the inverter control actions take place. The current injected in the grid depends on the receiving end complex voltage and apparent power. When the DG is inserted in the network the voltage .

2.3 Voltage Control using On-load Tap Changer (OLTC)

To ensure operating voltage is within the limits, voltage control in medium voltage network is achieved using on-load tap changers (OLTC) to regulate the voltage at the remote terminal [20]. The principle of operation of OLTC, voltage regulators and auto-transformer are similar. Figure 2.5 represents the schematic of OLTC transformer along with its equivalent circuit. The primary and secondary side are denoted by the notations p and s, where U, I, Z and n corresponds to voltage, current, impedance and turn ratio of the transformer respectively [17].The OLTC mechanism may be either on high voltage side or low voltage side. Usually, the tap changer are provided towards high voltage side as the current is low which makes it easier for switching the current following the concept of "make before break". Also, the availability of large number of turns help in achieving regulation with higher precision [21].

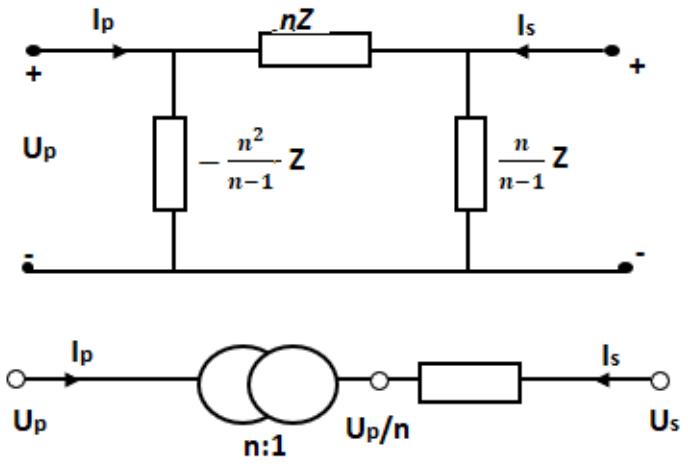

Figure 2.5: Schematic representation of OLTC with equivalent circuit [17]

The complex voltage flowing through the transformer can be expressed as in eq.(2.2) including the complex tap of the transformer as:

$$S_{PST} = V_P^2 t^2 (G_L + jB_L + Bsh) - V_P V_S (G_L + jB_L) te^- j(\theta_P - \theta_S + \phi t) \tag{2.8}$$

Figure 2.6 given in [20], [22] represents the basic control structure for regulating the bus voltage using OLTC with LDC (Line drop compensation). The bank current and bus ter-

minal voltage information is accessed using C.T. and P.T. The voltage drop is estimated by using the bank current, resistance and reactance from the transformer to the point where voltage is being regulated. The reference voltage set point is the midpoint of higher and lower voltage limits and is also know as "voltage band center".
The OLTC can also be performed without LDC. In such as case, the bank current is not required and the difference between bus voltage and reference voltage is eliminated by changing the tap position [6]. The voltage relationships can be written as :

$$U_{max} \geq U_{sig} \geq U_{min} \quad \text{and} \quad U_{sig} = U_{act} - U_{ref} = \begin{cases} positive, & \text{for overvoltage} \\ negative, & \text{for undervoltage} \end{cases} \tag{2.9}$$

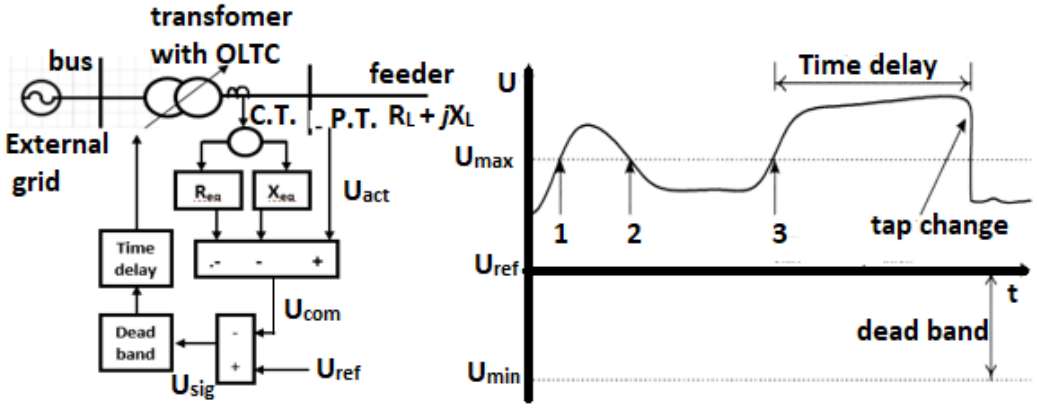

Figure 2.6: Control of voltage using on-load tap changing [20], [22]

In addition to this, an intentional time delay is provided prior to tap changing action when the voltage is "out of band" to avoid unnecessary changes during stable operation of the grid. Position 1 and 3 corresponds to counter start during which control mechanism is initiated. If the voltage is out of bandwidth for certain time delay, transformers tap position is altered otherwise counter stop is executed to stop the control action as shown by position 2.

In case for OLTC with LDC setting, the resistance and reactance setting can be obtained as [6]:

$$R_{eq} = \frac{N_{CT}}{N_{PT}} R_L \quad \text{and} \quad X_{eq} = \frac{N_{CT}}{N_{PT}} X_L \tag{2.10}$$

where = (N_{CT}) and (N_{PT}) are the turns ratio of C.T. and P.T. The load resistance (R_L) and reactance (X_L) represents the and feeder impedance connected to the transformer.

2.4 Voltage Control using DER Interfaced with Inverter

Taking into account the dependency on power production, the DER's interfaced with the grid at PCC can be enlisted in four categories: direct machine coupling, full power electronics, partial power electronics and modular or distributed power electronics interface

[23]. The most efficient is the direct machine coupling as it doesn't require any intermediate stage. For power generation with power electronic converter as intermediate stage, the type of category it belongs to depends on the size and type of power generation technology. The control strategies adopted for grid connected PV inverters can be broadly classified into two categories [24] (see figure 2.7).

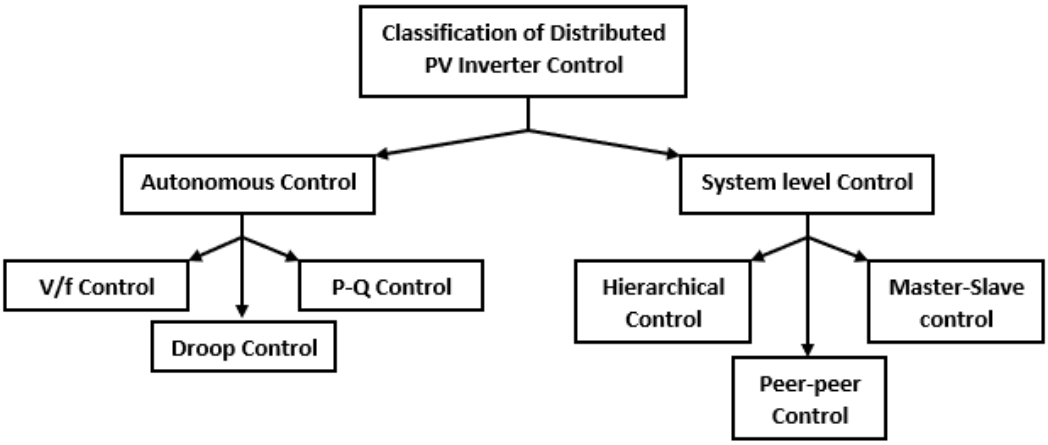

Figure 2.7: Classification of Distributed PV control

- **Autonomous/local Control**

Grid connected power electronics can be utilized to enhance flexible control for the stable system operation. This type control actions are generally fast as it involved controlling gate pulses of the power electronic switches which are operated at high frequencies. The inverter based DER's distributed throughout the network can be locally/internally controlled by three methods as suggested in [24]:
(i) V/f Control: In V/f control, the DER is modelled as a voltage source with a low series impedance. The inverter operates in grid-forming mode to maintain the voltage and frequency at desired set points. The active and reactive power exchanged with the grid depends on the system loading conditions. The local grid voltage and frequency are sensed and controlled actions are performed in closed loop manner. [24][25].
(ii) P-Q Control: In this control mode, the inverter is operated in greed-feeding mode i.e. a current source in parallel to a high impedance. The control actions are performed by obtaining the decoupled active and reactive power are controlled independently with respective to desired set points. Most of the DER fall under this category [25].
(iii)Droop Control: The droop control technique is a grid-supporting function which is among the popular choice of control for distributed power converters as they overcome the problem of load sharing when operating in parallel within a grid. They can be either operated separately or in combination with other two methods [26].

- **System-level Control**

The control strategies applied at system level fall under this category. Various equipment's are connected to distribution network which are used to operate the grid satisfactorily. This level of control can be broadly classified into following three categorize [24]:
(i)Master-Slave Control: In this type of control strategy, one of the converter is operated in V/f control mode to maintain the voltage and provide reference current to the other DER enabled as slaves. These converters are operated in P-Q mode enabling efficient decoupled active and reactive power control. The master of the slave can be determined in various ways as reported in [27].
(ii)Hierarchical Control: In this type of control, the command signals are generated according to network requirements at a central location (such as substations), which later communicated to the rest of inverters within the grid for executing necessary changes. They are also referred as centralized/ concentrated control. The major drawback associated with this method is if the central controller (master) fails to response, the control actions required won't be executed . These controls require common synchronisation signal and current sharing module which determines the reference current for each module with respect to load current [24], [27].

(iii)Peer-to-Peer Control: This type of control is also known as distributed control which has the properties of both autonomous control and centralized control. The control actions are initiated locally to control the bus voltage locally. However, control actions are also communicated through central level controllers when local control cannot regulate the bus voltage. When the local control is not sufficient, centralized control actions take place [28].

2.5 Solar Photovoltaic System

The solar power can be harnessed in many ways such as directly converting the solar irradiance into electricity using solar panel converting the energy from photons, hybrid plants, concentrated solar power plants (CSP),etc [29]. In this thesis the focus is mainly on the solar photovoltaic systems. The semiconductor cells also known as wafers are used in solar panel to produce photocurrent when exposed to solar irradiation.The power produced by the panel is in DC (or kW) which can be expressed in relation with solar irradiation as:.

$$P = \eta.A.S.FF \tag{2.11}$$

where η is the efficiency of solar panel which is generally ranges from 15% to 17%, FF is the fill factor which determines the quality of cell, S is the solar irradiation (in W/m^2) and A is the area of the collector. The PV panel are generally interface with inverter for converting the power from DC to AC.

2.6 Grid Codes

As discussed in section 2.4, the local or internal control of inverters should regulate the nominal system voltage which comply with the standards. The Danish grid code given in categorises various PV plants based on there rating according to which minimum functionality requirements are described as shown in Table **??**.

Control Actions	**PV power plant rating**			
	A2	**B**	**C**	**D**
	(11-50 kW)	**(0.05-1.5 MW)**	**(1.5-25 MW)**	**(>25 MW)**
Q control	Y	Y	Y	Y
Power factor Control	Y	Y	Y	Y
Voltage Controls	N	N	Y	Y
Automatic PF Control	Y	Y	N	N

The methods listed above mainly involves control of reactive power to obtain desired voltage level. The RMS voltage variation according to must be within $\pm 10\%$.
The Q control, a constant reactive power is specified at which the PV should operate. The active power is injected independent of reactive power. The set point for Q can be changed as er requirement [30]. The power factor operation controls reactive power in proportion to the active power. Many variants are available such as cos(ϕ)-P,cos(ϕ)-V, etc. [31]. In case of voltage control, the control function regulates the voltage at desired set point. The reactive power varies as a function of voltage. An intentional dead band may be provided which may restrict the change of reactive power when the voltage is within the specified bandwidth. In this thesis, Q-V droop control is used to regulate the voltage. This type of control requires local voltage control signal to vary the reactive power in proportion [28].

Chapter 3

Steady State Analysis of Medium Voltage Distribution Network

3.1 Modelling of MV Grid

A practical 20 kV MV network from a rural part of southern Germany which is derived by the CIGRE task force [12] for the European configuration is considered (see Fig. 3.1). The three phase feeders are considered to be balanced and the topology of the network can be changed by connecting the feeders using switches S1, S2 and S3 (see section 2.1).

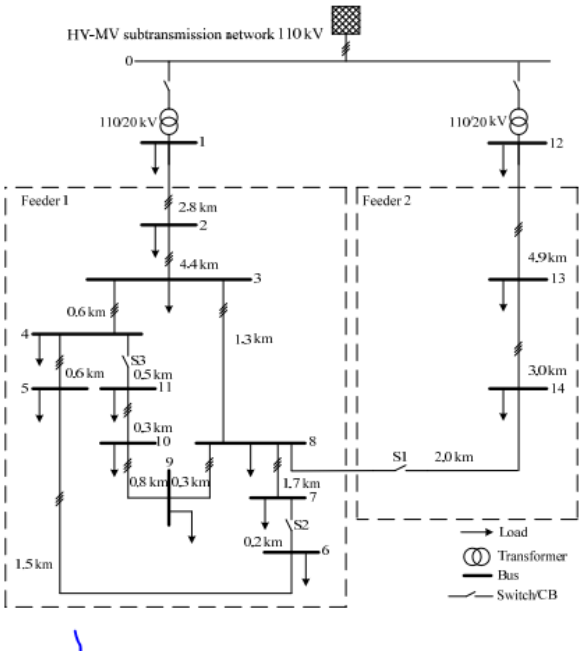

Figure 3.1: 20 kV CIGRE MV benchmark network

The 14-bus system consists of two feeders which are energised using an external grid connected at bus-0. The R/X ratio is 0.1 with short circuit capacity of 5000 MVA which suggests the network is very strong. Feeder-1 is mostly consists of underground cables (UC) while feeder-2 comprise of overhead lines (OHL). These distribution feeders also differ in their lengths resulting in different impedance between the nodes. The HV/MV transformers are of equal rating (25 MVA 110/20 kV) which are considered without tap change mechanism initially. There are two different kind of load present in the grid: residential and industrial. The loads are highest near the transformer on both the feeders. The related data obtained from [12] for modelling is given in Appendix A. The geometrical parameters for the conductors have not been taken into account. The performance of the grid is analyzed with all the switches (S1, S2 and S3) open i.e radial configuration.

In DigSilent PowerFactory, the load flow analysis is carried out using Newton-Raphson method. Feeder-1 and feeder-2 can be analyzed individually as all the switches and both are connected to each other via external grid which is considered as a slack bus in this case. All other remaining buses are considered as PQ bus or load bus as no generator is present at any bus present in the system. The Jacobian matrix relating the power mismatches to voltage (magnitude and phase angle) corrections are solved for each iteration for feeder can be expressed as [32]:

$$\begin{bmatrix} \Delta P \\ \Delta Q \end{bmatrix} = \begin{bmatrix} J_{P\theta} = \frac{\partial P}{\partial \theta} & J_{PV} = \frac{\partial P}{\partial V} \\ J_{Q\theta} = \frac{\partial Q}{\partial \theta} & J_{QV} = \frac{\partial Q}{\partial \theta V} \end{bmatrix} \begin{bmatrix} \Delta \theta \\ \Delta V \end{bmatrix} \tag{3.1}$$

where,

$$J_{P\theta} = \begin{cases} \frac{\partial P_i}{\theta i} = -Q_i \mid V_i^2 \mid B_{ii} \\ \frac{\partial P_i}{\partial \theta j} = - \mid V_i V_j Y_{ij} sin(\theta_{ij} - \theta_j - \theta_i) \end{cases} \tag{3.2}$$

$$J_{PV} = \begin{cases} \frac{\partial P_i}{V_i} = \frac{P_i + |V_i^2| G_{ii}}{V_i} \\ \frac{\partial P_i}{\partial \theta j} = \mid V_i V_j Y_{ij} cos(\theta_{ij} + \theta_j - \theta_i) \end{cases} \tag{3.3}$$

$$J_{Q\theta} = \begin{cases} \frac{\partial Q_i}{\theta i} = P_i \mid V_i^2 \mid G_{ii} \\ \frac{\partial Q_i}{\partial \theta j} = - \mid V_i V_j Y_{ij} cos(\theta_{ij} - \theta_j - \theta_i) \end{cases} \tag{3.4}$$

$$J_{QV} = \begin{cases} \frac{\partial Q_i}{V_i} = \frac{Q_i + |V_i^2| B_{ii}}{V_i} \\ \frac{\partial P_i}{\partial \theta j} = \mid V_i V_j Y_{ij} cos(\theta_{ij} + \theta_j - \theta_i) \end{cases} \tag{3.5}$$

The diagonal and off diagonal elements of eq. (3.23.5) represent the change in real and reactive power flow injection at a particular node with respect to voltage magnitude and angle at each bus [14]. The nodal power injections are the sum of all the line flow connected to it as given in eq. (2.102.8). Figure (3.2) represents the voltage magnitude of each bus in the system. As the voltage magnitude of feeder-2 is close to 1 .p.u. its not considered in this work. It can be inferred in most of the distribution lines of feeder-1 the voltage magnitude difference is quite low due to which voltage drop along all the feeders are quite low. Line 1-2 and line 2-3 which carry the total current delivering to bus-4, bus-8 and to the load connected at bus-3 have significantly higher voltage drop. Comparatively, voltage drop in Line 2-3 is higher as its length is greater than line 1-2 (see Appendix **??**) The voltage drop

across Line 1-2 is lower as compared to Line 2-3. This is because of absence of load at bus-2. The bus voltage deviation is minimal near the source as the R/X ratio of transformer is very less compared to the distribution feeder [28]. The voltage drop the rest of lines is quite low as the apparent power rating loads present within the system from bus-4 to bus-11. Hence deviation of voltage with respect to its sending voltage is quite low.

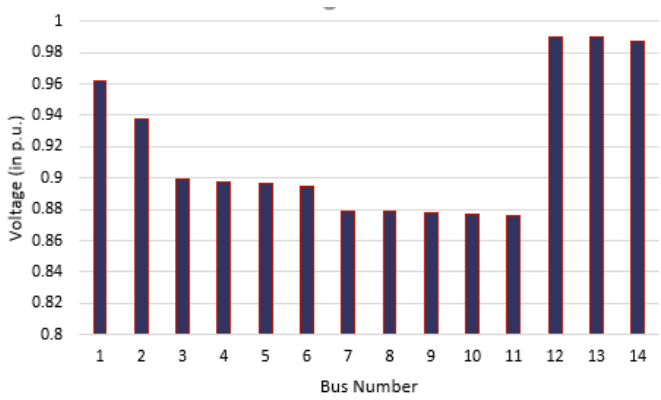

Figure 3.2: Voltage drop across lines in feeder-1

3.2 Sensitivity Analysis of Grid

The sensitivity coefficients often are used for associating the static scenario to the grid to control logic using linearized power flow. The Jacobian sub-matrices can be utilized to formulate the voltage sensitivity coefficients. For instance to derive the Q-V sensitivity relation, we set ΔP=0 and rewrite eq. (3.1) as:)[33][14]:

$$\frac{\Delta V}{\Delta Q} = (J_{PV} - J_{Q\theta} J_{P\theta^{-1}} J_{PV})^{-1} \tag{3.6}$$

Similarly, the expression can be obtained for V-P sensitivity can be obtained by setting $\Delta Q = 0$:

$$\frac{\Delta V}{\Delta P} = (J_{PV} - J_{P\theta} J_{Q\theta^{-1}} J_{QV})^{-1} \tag{3.7}$$

It can be seen that in every sensitivity relation, all the Jacobian sub-matrices are present. The diagonal elements of eq. (3.6 and3.7) represent the change in real and reactive power flow injection at a particular node will cause deviation of its nodal voltage. Similarly, variation of voltage due to power injection at another node can be calculated. [14]. Appendix A enlists the the sensitivity relations of each bus with respect to each other in matrix form (for both dV/dQ and dV/dP) for feeder-1. The sensitivity of feeder-2 is quite low due to which it is not considered in this project. It can be observed that the tail end of the feeder has very high sensitivities as compared to the nodes located near the transformer. Higher value of sensitivity indicated the consumer located at the feeder end has greater flexibility for power production. It should also be noted that the sensitivity relations of bus-7 to bus-11 are quite similar and very high compared to rest of the network. Bus-8 also have sensitivity similar to bus-9, however the difference with bus-7 is comparable. Bus-4

to bus-6 have similar sensitivity but is quite low as compared to bus 7-11. Bus-3 belongs to separate category as its sensitivity are different from the rest of the nodes within the feeder. The sensitivity of bus-1 and bus-2 are very low suggesting lack of flexibility for the consumers located near the transformer. Similar behaviour is observed for V-Q sensitivity however, the dependence of voltage deviation on reactive power change is higher than dV/dP sensitivity. This is because the reactance of the feeder is quite higher than the resistance. From this observation, feeder-1 is categorised in three different zones as shown in figure x. As the sensitivities of bus-3 and bus-8 are different from the rest of the network, they are excluded out of all the zones. Another reason for excluding these buses are the number of feeder connections at these buses are higher due to which effect of variation of voltage will be different.

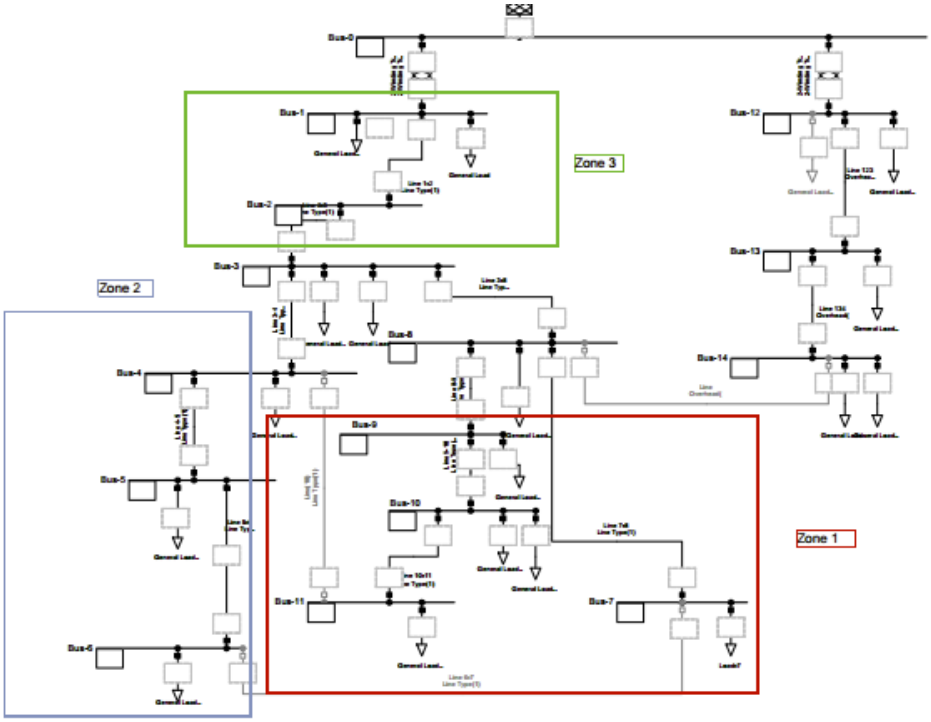

Figure 3.3: Different zones in the feeder based on sensitivity

The total voltage magnitude variation at any node (say bus-i) cause by the active power injection of PV at any number of given bus will be given by:

$$\Delta V_i = \frac{\Delta V_i}{\Delta P_i} + \sum_{j=1,\neq i}^{N} \frac{\Delta V_i}{\Delta P_j} \tag{3.8}$$

where N is the number of buses present in the feeder. When the number of solar PV increase in the grid, the magnitude rise will also increase. If the PV is injecting reactive power, dV/dQ sensitivity should also be taken account. A comparative analysis is required to analyze how much change in voltage is observed when the presence of PV increases in

the feeder. Hence an investigation regarding number of PV and their effect on bus voltage 11 is necessary which will be performed in the next section.

3.3 Analysis of DER Indices

The impact of DER of the network can be quantified using DER indices as suggested in [34][35]. The choice of DER generally depends on the type of analysis and parameters under consideration. In our case we are interested in voltage control. The penetration level is the ratio of amount of power generated from the DER to the power consumed by the total load demand within the grid [34].This is an important aspect for analyzing the DER behaviour as the consumer or DER owner would invest depending on the load requirement. However, it only takes into account real power only given as:

$$\%DG \quad Penetration = \frac{P_{DER}}{P_L} * 100 \tag{3.9}$$

where P_{DER} is the total active power of the DER connected within the grid and P_L is the total load of the system during a specific time. Similarly, dispersion factor measures the amount of nodes within a system that are connected to DER. It is given by the ratio of number of buses connected with DG to number of buses where loads are located [34].

$$\%Dispersion \quad Level = \frac{No.of BuswithDG}{No.of BuswithoutDG} * 100 \tag{3.10}$$

Let us consider a scenario in which DER are injected based on their sensitivity (from high to low). This will allow us to see more large variation as the sensitivity of bus 7-11 are higher (see fig. 3.2) which might lead to undesirable circumstances.It is assumed that the penetration level is shared equally when two or more PV's are connected with the grid. It is also assumed that all the DER are operating at unity power factor. In practical scenario, it might not be the case but this base case can be used to understand the behaviour of the grid during quasi-dynamic conditions. The penetration level is taken at every 10 % interval with increasing dispersion level in feeder-1.

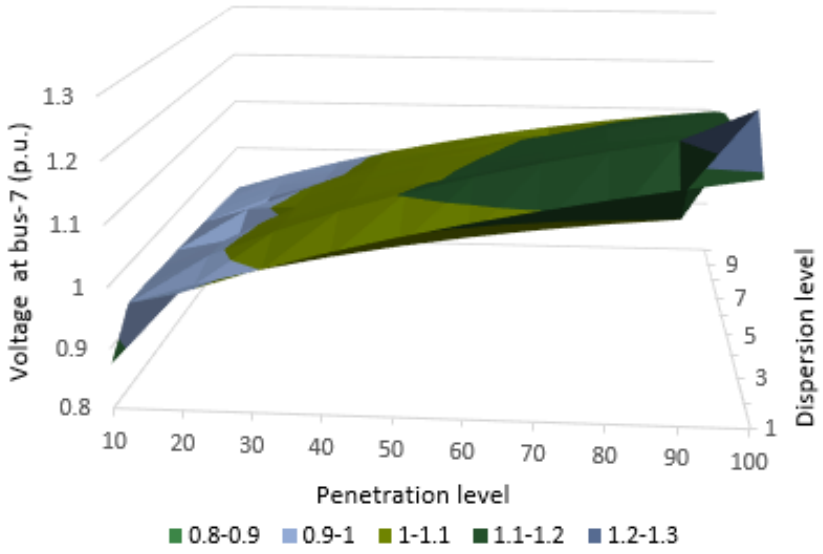

Figure 3.4: Variation of IVD with penetration and dispersion level

It can be seen from the figure that any increase in penetration level (or increment in real power) results in increase of voltage. At low penetration level, the voltage magnitude decreases with simultaneous increase of dispersion level. This is because the sum of all the sensitivity contributing to voltage change has lower power injections which causes a voltage change lower as compared to power injection with less dispersion level. from At very high penetration level (80-100) the voltage magnitude first increases to certain extent and then starts to decline. This suggests that the superimposed effect of dispersed DER causing voltage change is higher compared to changes caused by DER present at bus-7 only for same penetration level. When the dispersion level is further increased this superimposed effect again reduces causing voltage to reduce.

3.4 Chapter Summary

In this chapter, a steady state investigation is performed to analyze the grid under consideration. The grid was operated in radial topology which resulted in considerable voltage drop from the external grid to the end. In the next section, sensitivity analysis was performed providing insights about changing voltage magnitude and angle with respect to active and reactive power. It was seen that that weak buses located at end of feeder-1 has higher sensitivity which might will cause considerable voltage deviation in presence of DER as shown in the analysis of DER indices. With increasing penetration and dispersion level it is necessary to keep the bus voltage in regular check as intermittent nature of DER would produce considerable voltage changes.

Chapter 4

Effect of Solar PV and OLTC on Voltage Control

4.1 Generation and load profiles

The power system phenomenon can be analyzed at various time scales ranging from microseconds to years or decade. Interaction of time varying PV source with other time varying parameters which may or may not be controlled is essential for defining a control strategy. Figure 4.1 demonstrates various areas of consideration at different time scales. Analyzing the complete spectrum of operation would require excessive amount of data and computation time would also increase. [36].

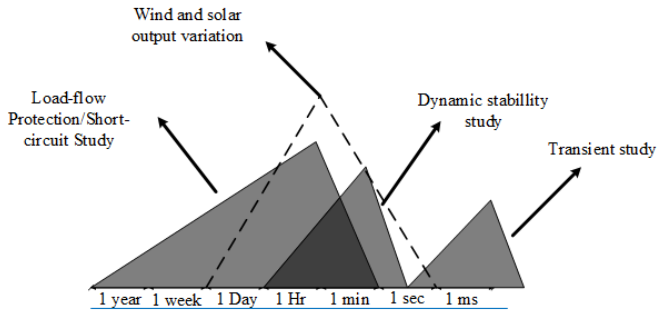

Figure 4.1: Power system phenomenon vs Time scale

In this thesis, the available solar radiation data is taken at 30 minutes interval from which the PV power injection can be calculated using eq. (4.2) as shown (see figure **??**). The available load data (see figure 4.3) is given in p.u. at every 1 hour interval. The solar power profile is considered same for all the PV's present in the grid. Similarly, the load profile is also used for both the loads (i.e. industrial and residential) at each bus. However, due to the different apparent power rating the consumption of power will differ at each node at any point of time.

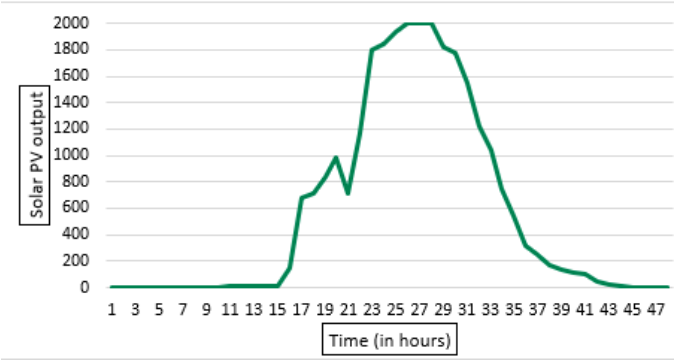

Figure 4.2: Daily Solar Power Generation

As discussed in section 3.3, with the increase in dispersion level, the power injection into the grid can be increased. Hence, it is assumed that generation of power exist at all the consumption nodes (i.e. dispersion level of feeder-1 is 10/11).

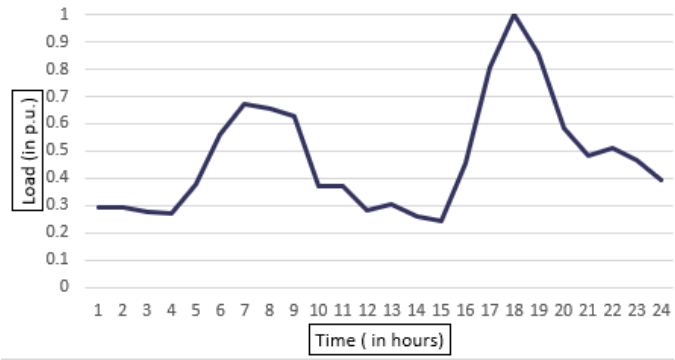

Figure 4.3: Daily Load Profile

4.2 Operation of OLTC control

In this section, analysis of grid voltage behaviour with OLTC control is carried out. The PV is operated at unity power factor and does not take part in voltage control by absorbing or injecting reactive power within the system. The magnitude of voltage change with each tap is generally expressed in percentage of winding voltage. The specification that are used is given in [12] (see Appendix **??**). The tap can be altered ± 10 from its neutral position. It is required to regulate to voltage within $\pm 10\%$ As the transformer belongs to Dyn1 vector, the phase shift provided by the transformer is 30 deg(lag). The remote bus which are selected are categorized in various scenarios given in Table (4.1).

Figure 4.4 represents the variation of voltage at bus-11 (most sensitive bus) for all the case scenarios. The load consumption between 00:00 and 6:00 increases from 0.2 p.u. to 0.67 p.u. The PV power output is almost zero as the solar radiation is almost negligible during this interval. The voltage varies near 1 p.u. and the voltage at bus-11 with or without control is same. No tap change action is initiated during this interval in any

Case Scenarios	Remote locations
Case I	No OLTC operation
Case II	OLTC operation in Zone-1
Case III	OLTC operation in Zone-2
Case IV	OLTC operation at bus-8
Case V	OLTC operation at bus-3

Table 4.1: Case scenarios for remote OLTC operation

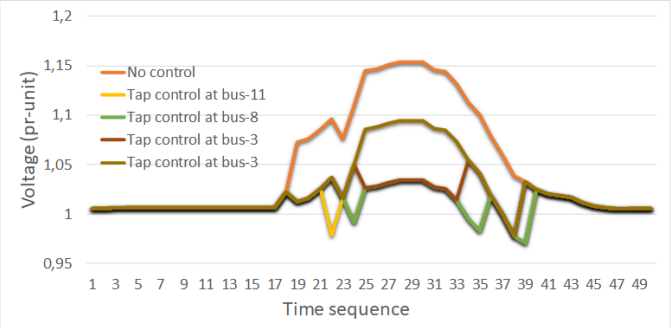

Figure 4.4: Voltage magnitude at bus-11 for all scenarios

case. When the solar power production begins at 7:00 and reaches to a value of 670 kW at 9:30, and the load consumption starts reducing and reaches a value 0f 0.2 p.u during the same time period. The tap position is altered in each case (except case I) and is set at -1 as shown in figure (4.5). When the tap position is lowered, the voltage at bus-1 is reduced which in turn reduces the voltage level of the whole system such that the nodal voltage at the controlled is within ± 10. However, it should be noted that the magnitude of voltage change at each bus will be different and the effect on voltage magnitude due to transformer tap is least at the weakest bus. This is due to the increasing impedance with increasing line length from transformer to remote bus. Hence, the voltage rise due to PV penetration is therefore mitigated and instead of voltage rising to a higher value. Further it is noticed that for case II, an additional tap variation is observed between 9:00 and 10:00 where tap position is set to -2 at 9:30. During this interval, the shift of load consumption from 0.6 p.u to 0.4 p.u increases the voltage magnitude. Although there is a sudden drop of PV penetration which may be due to variation of climate or other factors, the resultant change results in voltage rise. This results in additional change of tap when compared to other cases. At 10:30, the solar radiation becomes evidently high which causes the voltage to rise beyond the maximum threshold voltage. At this the tap position is set to -2 in all scenarios except for case V which is set at -1. This is because the maximum voltage magnitude at bus-3 is lower than rest of the buses under consideration.It should be noted that the tap change initiated in case IV is earlier than in case III. this is because the the sum of sensitivities effecting bus-8 is higher than bus-6 (in zone-1). From 11:00 to 15:00 the tap position remains fixed for all the cases except case I and case V. The PV power increases and attains a maximum value of 2MW during this interval with simultaneous decline in load

consumption which reaches a value of 0.2 p.u. The PV power production starts declining

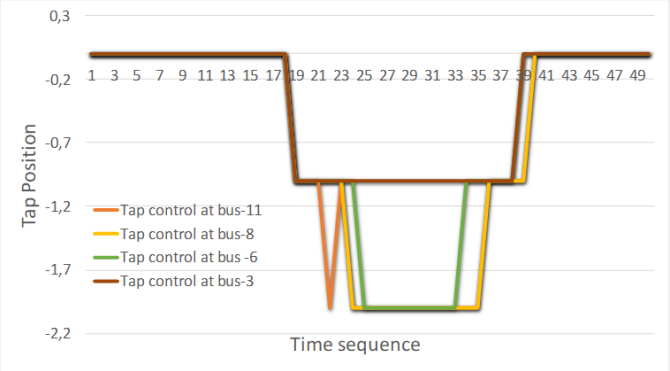

Figure 4.5: Variation of tap position

at 15:00 along with increment in load consumption. At this point the voltage magnitude at bus-6 starts declining and the tap position is shifted to -1 position for Case-4. However, for Case-3 and Case-2 the voltage magnitude is still out of limit and tap position remains at 2. At 15:30, the further decrease in PV power decreases the voltage magnitude at bus-8 also which allows the tap position to return at -1.This action continues with decreasing PV until the voltage magnitude at bus-8 reaches within limit (at 16:00) and when the PV generation, becomes reduces at night, all the tap positions are adjusted back to its neutral position. It should be noted that Case-5 operation shows only single tap position change which lasts from 8:00 to 17:30. The OLTC operation time is highest for bus-11 and the least for Case 3 and 4 both. Also, the OLTC performance for any other bus belonging to that particular zone will have a similar tap response. However, the voltage magnitude may differ a bit which is insignificant to cause any other kind of variation. As discussed

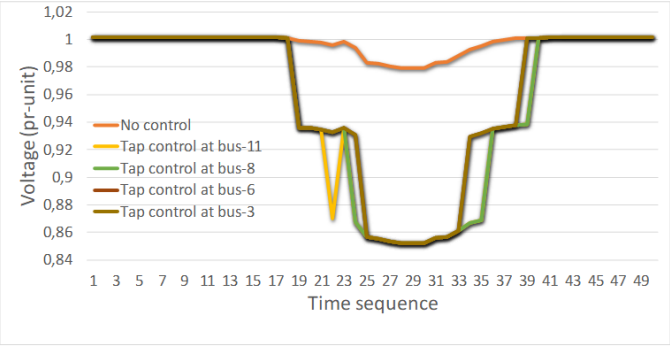

Figure 4.6: Voltage magnitude at bus-1 for all scenarios

above, the remote control operation of OLTC will regulate its low voltage terminal voltage to compensate the voltage. Figure **??**resents bus-1 voltage for all the cases. It can be seen that the voltage magnitude drops below 0.9 p.u. during the interval when PV is producing power at its rated capacity. Thus, the voltage regulation achieved through remote control OLTC operation is insufficient for the duration 10:00 to 16:30. The undervoltage condition

at bus-1 results in undesirable operation. This suggests that remote control operation of OLTC in each case requires other measures to control the voltage magnitude of the system within $\pm 10\%$.

4.3 Q-V Droop Control of PV inverter

In the section, emphasis is given on utilization of PV inverter reactive power capability without OLTC control. First, the apparent power rating of the inverter of the PV is to be determined. In our case, it is assumed to be equal to rated power produced by PV i.e rating of inverter is 2MVA. The maximum reactive power injection ability is taken to be 44% of the MVA name plate rating(i.e. $Q_{rated} = 0.968MVAR$). In other words, the power factor at which the PV can operate should lie within 0.9 (leading and lagging) when operating at its rated kVA as suggested in the grid codes [30]. However, the power factor rating is chosen to be unity as the consumer would like to extract all the power produced from the PV panel. Thus, it is required to utilize the available capacity without effecting the real power generation. Therefore, in this thesis Q-V droop control technique is used. (**??**).

Figure (4.7). shows a typical Q-V characteristics as given in [37]. When the voltage is within the specified limits (V_2V_3), no reactive power support is provided by the PV. When the voltage is less then minimum voltage of the specified band, the reactive power is injected into the system based on the operating voltage and droop setting (vice versa for over-voltage). The droop setting is usually provided by the DSO, therefore it's impact on the performance of the grid must be investigated. The specifications provided in [37] is used for calculating droop setting (V3=1.02 and V4=1.08).

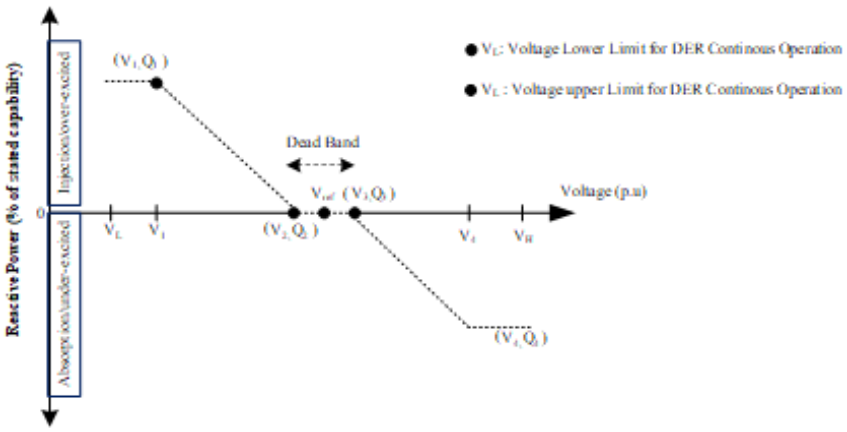

Figure 4.7: Q-V droop characteristic for PV system [37]

The rated reactive power delivered by any PV in the system is fixed (Q_{max}). The droop settings in case of overvoltage can be calculated as [28]:

$$m = \frac{Q_1 - Q_2}{V_1 - V_2} \tag{4.1}$$

Voltage-Reactive power parameters	Default Settings	Allowable Setting Range	
		Min	Max
V_{ref}	V_N	$0.95V_N$	$1.05V_N$
$V_1 and V_4$	$V_{ref} \pm 0.08$	$V_{ref} - 0.18V_N$	$V_1 = V_{ref}$ $V_4 = V_{ref} + 0.18V_N$
$Q_1 and Q_4$	44% of MVA rating	0	100 % of MVA rating
$V_2 and V_3$	$V_{ref} \pm 0.02$	0	$V_2 = V_{ref} - 0.03V_N$ $V_3 = V_{ref}$
$Q_2 and Q_3$	44% of MVA rating	0	100% of kVA rating

As the voltage magnitude limit is 1.02 for overvoltage condition, the voltage control will be initiated prior to OLTC control which is operated at $\pm 10\%$. Therefore, the operation of voltage control will be initiated prior to tap control operation with rise in voltage magnitude beyond the given range.
Figure **??** represents variation of voltage magnitude in zone-1 (at bus-11), zone-2 (at bus-6), bus-3 and bus-8. At 7:30, when the solar PV generation is increasing with the sunrise, the voltage magnitudes in Zone-1 reaches to a value above 1.02 the PV in Zone-1 as well as PV at bus-8 starts absorbing reactive power to bring the voltage at its set point (except for PV at bus-1). As the generation increases and load decreases simultaneously the voltage keeps rising and the reactive power absorption is increased. Although, the voltage profile shape is almost same, the magnitude differs when the reactive power absorption starts. The reactive power absorption to for each PV is shown in fig 4.8(except PV at Bus-1).

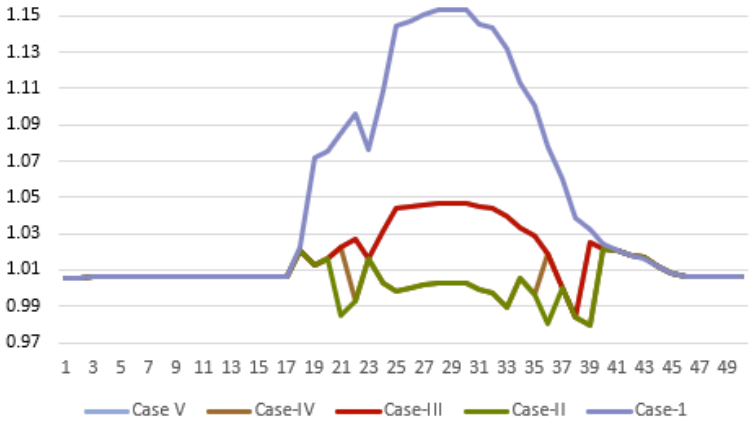

Figure 4.8: Voltage magnitude at bus-11 with and without Q-V control

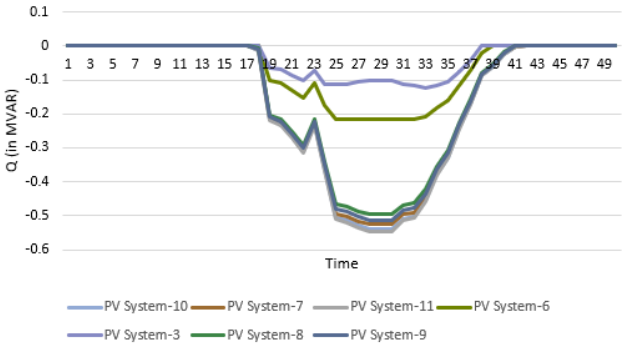

Figure 4.9: Reactive power consumption of solar PV system

The reactive power absorption is different for all the PV's. However, PV's located in each zone has almost similar consumption. This is because identical droop settings has been considered at each bus along with the effect of feeder impedance.. The injection of active power and simultaneous consumption of reactive power by the PV can cause overloading of the inverter.

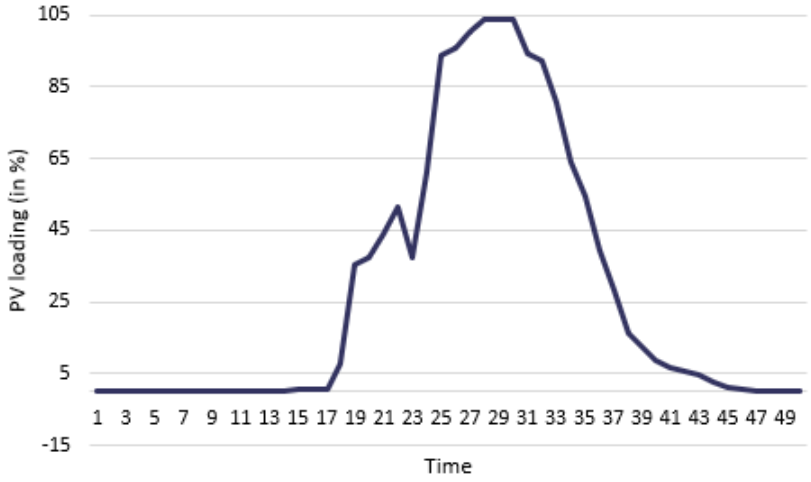

Figure 4.10: Loading of PV

Figure **??** and figure **??** represents the loading of PV located at bus-3, bus-8 and bus in Zone-1 and 2 with and without droop control.During the interval 12:00 to 13:30, the loading of PV in zone-1 exceeds 100% as the PV power production reaches it rated value (2MW). Also the voltage magnitude is high during this interval which result in absorption of reactive power.

4.4 Chapter summary

In this chapter, the effect of OLTC control Q-V droop control is analyzed individually. First the OLTC operation was investigated which is controlling the remote bus in each

zone along with bus-3 and bus-8. It was observed that the number of tap actions is higher in the zone-1 and the least when OLTC is operated at bus-3. Also, the tap position is changed to -1 in case of bus-3 compared to -2 in case of zone-1. The effect on tap change was similar for zone-2 and bus-8. However, the duration of tap change is reduced by an hour. The voltage was although regulated at the remote in each case, undervoltage at bus-1 was observed which was beyond $\pm 10\%$ range. In the next section, Q-V droop control was used in which nominal settings were used for all PV (except at bus-1). The voltage control performed by the Q-V control restricts all the bus voltage magnitude within the limits including bus-1. However, the voltage magnitude in zone-1 and 2 was higher as compared to OLTC tap change. The reactive power consumption was maximum at the weakest bus and least at bus-3. However, for small duration overloading of the PV system was observed when the active power generation is at its peak.

Chapter 5

Voltage control using OLTC and Droop Control

5.1 Uncoordinated control of OLTC and Q-V control

In this section, the effect of OLTC remote control for different cases in presence of Q-V control performed by the solar PV is analysed. The simultaneous control of voltage by PV and OLTC operating at different voltage control set points (voltage ref. is same i.e. 1 p.u.) have an adverse effect on the system. The simulations are analyzed based on the scenarios as given in table 4.1. Figure 5.1 represents the variation of voltage magnitude at bus-11. It can be inferred that the voltage during each operation is quite low in all the cases as compared to voltage control by OLTC and Q-V control individually (see Fig 4.4 4.8). The OLTC tap position is significantly effected to due presence of PV voltage control. The range of tap change is increased from -2 to -3 as shown in figure 5.2. The variation of tap change for case-II and case-IV become quite similar. However, the tap change initiated in case of case-IV is delayed by 30 minutes after which the voltage at bus-8 is regulated. However in case of control performed only OLTC, the variation was similar to as case-III characteristics. Case-V remains unaffected and the maximum tap position attained is -1.

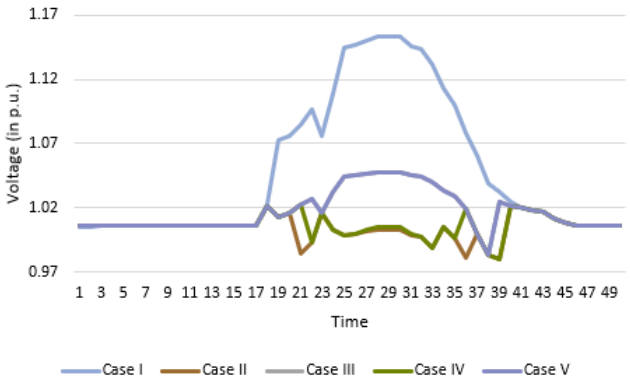

Figure 5.1: Voltage magnitude at Bus-11 for each case

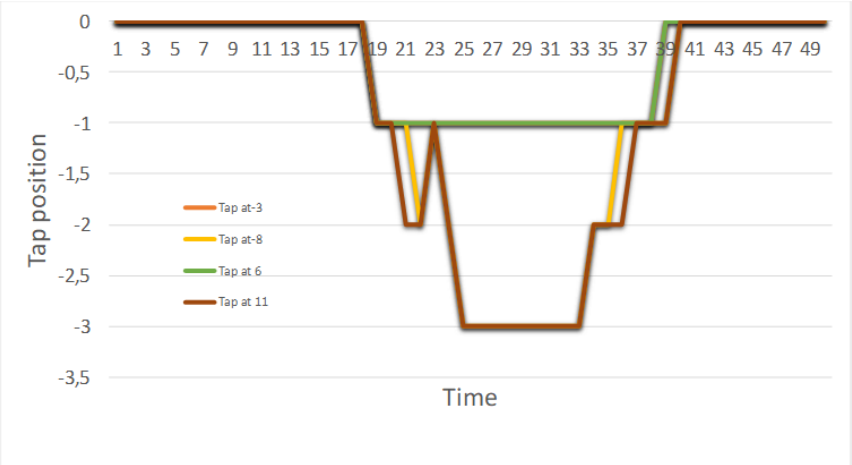

Figure 5.2: Tap position of OLTC

The change in tap position also effects the voltage at transformer secondary terminal. The worst case is observed when the transformer is regulating voltage at bus-11. Similar behaviour was observed when only OLTC was operating. However in this case the voltage magnitude drop considerably low at a value of 0.8 p.u. Figure 5.3 represents the variation of voltage magnitude at bus-1. The voltage magnitude variation at all the other buses will be within the variation of bus-1 and bus-11 (least and most sensitive bus). This increase of voltage tap resulting change in voltage which are undesirable is due to the participation of solar PV in voltage control. The reactive power variation in this scenario is different

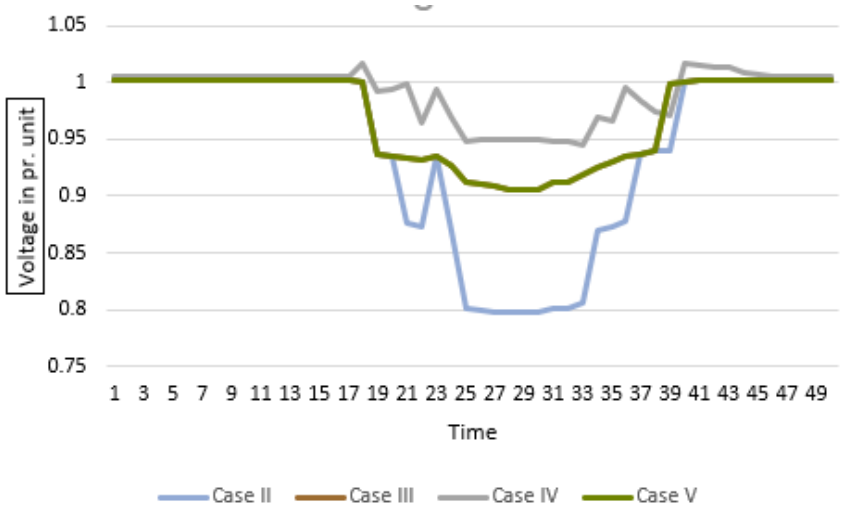

Figure 5.3: Voltage magnitude at bus-1 for all case scenarios

from the Q-V control. The participation of of PV's located in zone-1 and bus-8 is almost negligible. Figure 5.4 and 5.6 represents the reactive power variation for case II and case V respectively. As the tap variation of case IV and case II were similar, the reactive power

generated or absorbed by the PV is indistinguishable. Similarly, case II and case IV also have similar behaviour. The reactive power is injected to the grid when OLTC is operating at bus-1. Due to tap change mechanism, the voltage at bus-1 and bus-3 reduces below 0.98. The operating characteristics provided is required to inject reactive power when the voltage reduces below 0.98 p.u. As the tap change increases the reactive power also increases

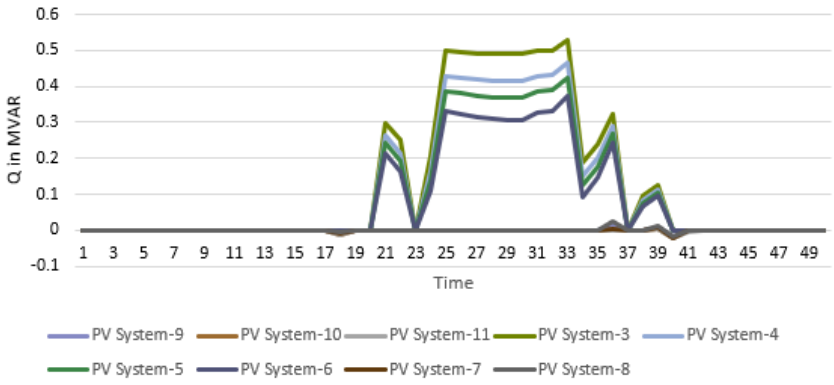

Figure 5.4: Reactive power variation of PV for case II

and reaches to a value of 0.5 MVAR. Due to this additional reactive power injection, the tap position reaches a maximum value of -3. However, while simulating case II, the reactive power is being absorbed and reaches a maximum value with change when the tap position is set to maximum. The injection or absorption of reactive power is higher for PV located at bus-3 than any other bus. This is due to the fact that bus-3 is located near the transformer secondary terminal and as the voltage tap is reduced, the voltage magnitude at bus-3 also reduces. When the voltage will be minimal at all time in presence of OLTC control. Due to which reactive power is injected to provide voltage support. In case V,

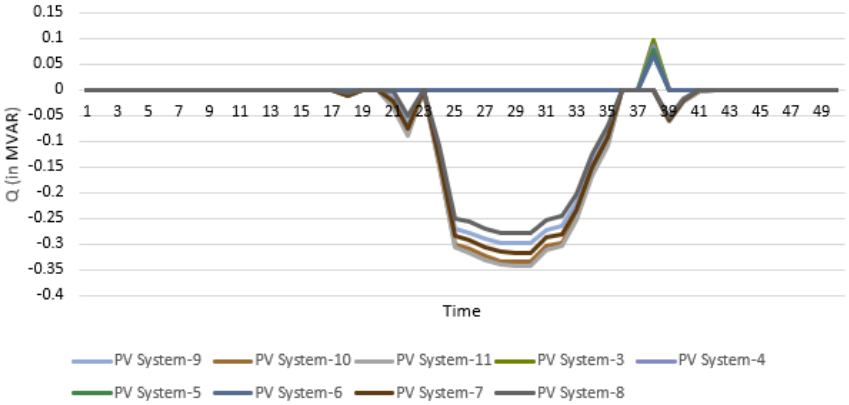

Figure 5.5: Reactive power variation of PV for case-V

the reactive power variation is similar to the scenario when only Q-V droop is operated. However, it should be noted that in case, the magnitude of reactive power absorbed is reduced. Also, PV located in Zone-1 and bus-3 do not take part in voltage control. Since

the real power produced is unaffected, the loading of PV inverter increases beyond 100% during maximum power production. Figure 5.6 represents the loading of PV located at bus-3. Since the power absorbed or injected by any PV in the bus is lower. It is evident

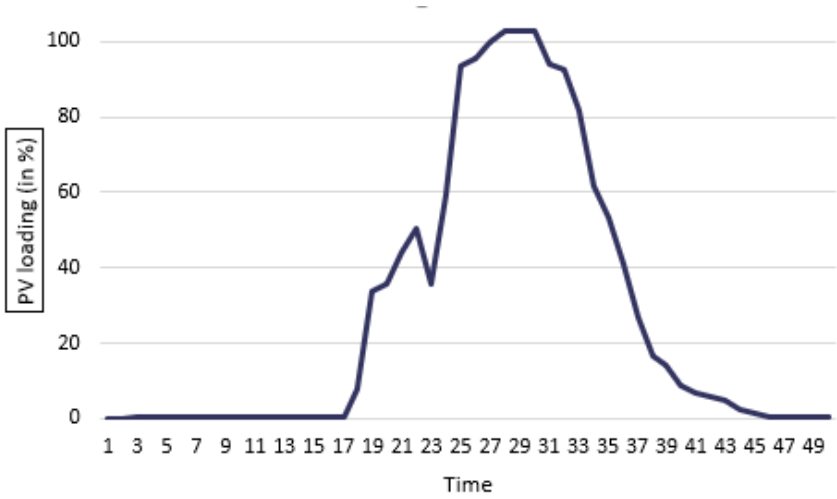

Figure 5.6: Loading of PV at bus-3

from the above discussion that the control of OLTC along with Q-V droop control has to be coordinated. The number of tap changes along with the maximum tap position.

5.2 Coordinated control of OLTC and PV droop control

This section describes the control strategy adopted for maintaining all the bus voltage in feeder-1 within the $\pm 10\%$ voltage range is discussed. Distributed control techniques is used which has the features of both centralized control and autonomous control as discussed in 2.4. In this case the OLTC is operated as a centralized controller due to which the remote control operation is performed simultaneously at all the buses integrated with PV source. As the objective of this thesis is to minimize the tap change ensuring voltage within prescribed limits. Figure 5.7 represents the control block diagram according to which the Q-V control and OLTC control are coordinated for optimum voltage control.
The control action is initiated by comparing the actual voltage with dead band provided in the Q-V control (1.02 p.u.). If the voltage is within the limits no control is initiated. As the voltage increase beyond the limit, the PV is required to regulated the bus voltage if the reactive power capacity is available from the inverter. When there is further increase in the voltage which cannot be regulated by PV, then tap change is initiated. However, the tap position must lie within the specified range. As the OLTC is regulating bus voltage within $\pm 10\%$, the actual voltage is compared with the upper voltage band. If the tap position is not available or the bus voltage is less than 1.1 p.u., the voltage check for Q-V characteristics is initiated. This closed operation will allow the controllers to maintain the voltage within permissible value.

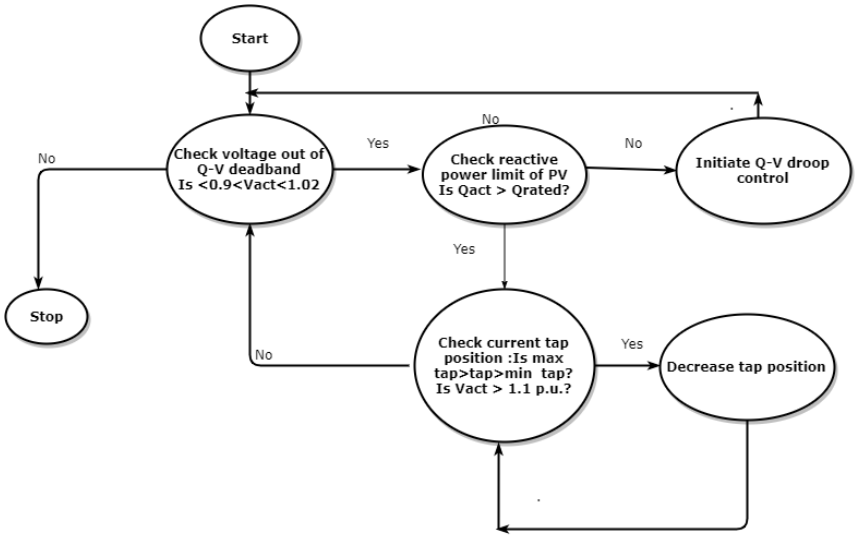

Figure 5.7: Control for coordination of OLTC and Q-V droop control

Figure 5.8 represent the variation of voltage magnitude of bus-1 and bus-11. It is evident that the voltage magnitude reaches maximum value of 1.05 at bus-11 while bus-1 voltage reaches up to 0.9. It should be noted that in this case the voltage at all the buses are within $\pm$10% range where the voltage magnitudes lie between bus-1 and bus-11.

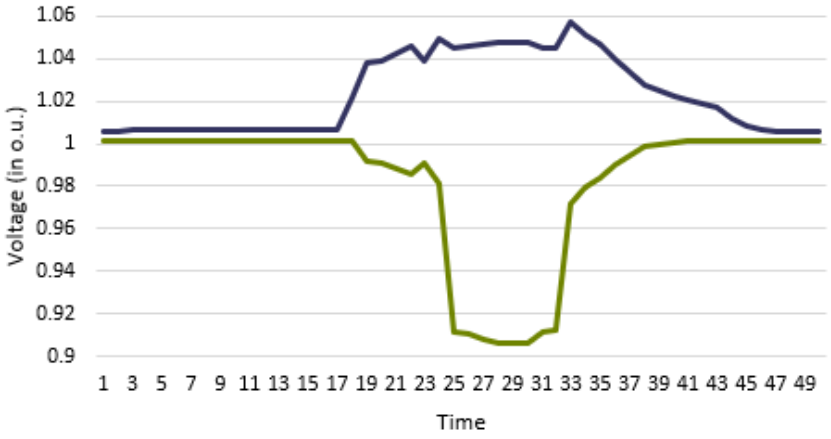

Figure 5.8: Voltage magnitude at bus-1 and bus-11

The PV inverter at any bus absorbs reactive power as soon as voltage reaches beyond 1.02 p.u. The Q-V control will bring back the voltage back to its voltage set point point value depending upon the availability of reactive power capability. When the voltage rise is significant, the Q-V control alone is not sufficient to bring the voltage within limits. Due to this tap change is initiated by the transformer as shown in figure5.9. It should be noted that voltage is brought in limits by changing tap position at -1. During this interval, PV

power production reaches to maximum value. When the real power injection is reduced the tap position is positioned back to neutral position.

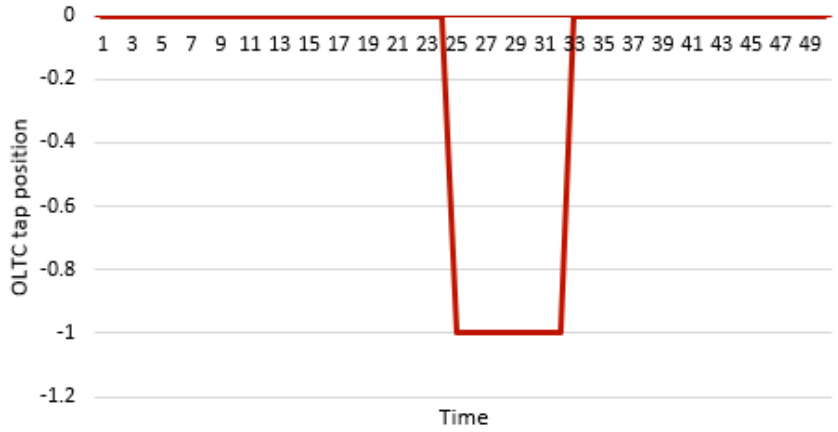

Figure 5.9: Tap position of OLTC

Figure 5.10 represents the variation of reactive power of all the PV enabled with Q-V control. It should be noted that all the PV are contributing in voltage control by absorbing reactive power. However, the reactive power absorbed at each node by the PV is different. This is because the sensitivity of all the buses are different. Due to this rise of voltage magnitude in zone-2, bus-3 and bus-8 is comparatively lower than the voltage at bus-11. The reactive power absorption begin as the PV power rises.

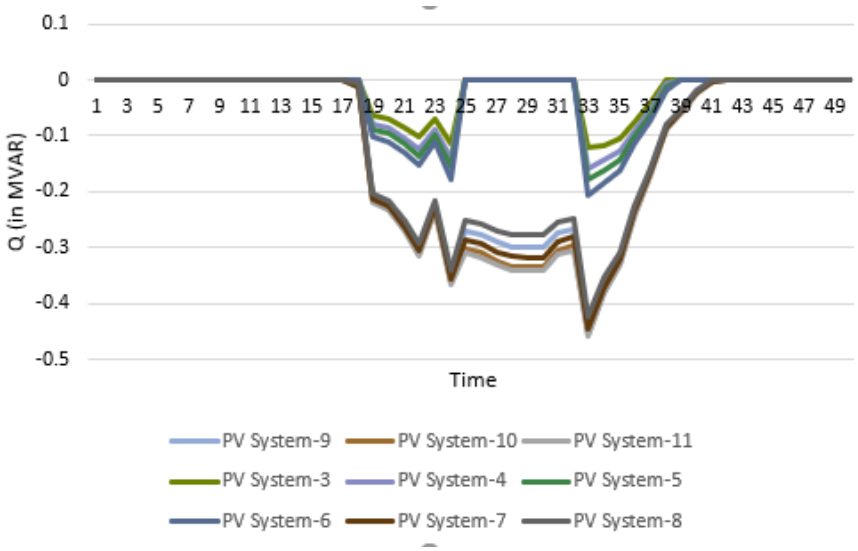

Figure 5.10: Reactive power output for PV with Q-V control

When the voltage magnitude further increases the tap action is initiated. As the voltage is reduced due to the tap action, reactive power absorbed by the PV reduces (injected

back into the grid). This results in less loading of PV inverter (around 101%) which is comparatively lower compared to uncoordinated control. The loading of transformer is

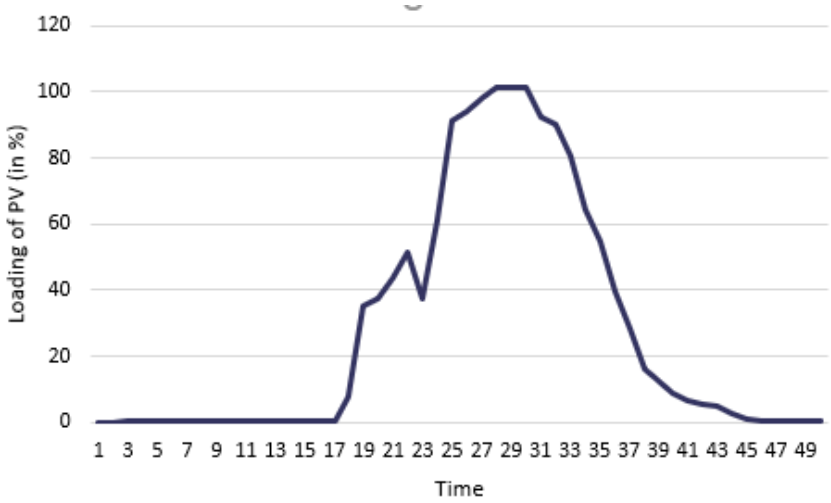

Figure 5.11: Loading of PV at bus-11

maximum for PV at bus-11 as the reactive power absorbed is higher than any other PV within the network. Figure 5.11 represents the loading of PV.

5.3 Chapter Summary

In this chapter evaluation of coordinated control of active distribution network in comparison to uncoordinated control of OLTC and PV droop control (Q-V). From the results obtained, it is clear that number of tap change is reduced from 1 to 3. Also, the maximum tap deviation is reduced as the PV operates at maximum position of -1. The reactive power absorbed or generated by the PV depends on the PV location and the remote bus selected for regulating the voltage. The loading of the PV is also reduced to a certain extent. However, it is impossible to reduce the loading below 100% during peak interval as the real power produced by the PV is equal to MVA rating of the PV.

Chapter 6

Conclusions and Future Work

6.1 Conclusions

In this thesis fundamental principles are worked out which are generally used in voltage control. With the rising solar PV system in the grid, effective management using coordinated control is developed. At first the MV grid is analyzed using sensitivity analysis. Based on the sensitivity relation of each bus different zones were established. Bus-3 and bus-8 were considered individually as their sensitivities were different from buses in any zone. The consumers should be allowed to integrate PV system with the grid to increase competitiveness in the market. Hence, an investigation was carried out varying dispersion and penetration level. It was observed that with increase of dispersion level the maximum allowed power injection can be increased significantly. However, when the same power is produced with less dispersion level, the voltage magnitude increases.
In the next chapter OLTC control is used for regulating the bus voltage in the active distribution network. Remote control in the defined zones as well as at bu-3 and bus-8 were investigated. It was observed that when bus-3 is regulated the number of tap changed required is less. Regulating the weakest bus results in undervoltage at bus-1. Selecting any bus within the zone will result in similar behavior in voltage magnitude variation. In the next section Q-V droop control technique was used. The voltage bandwidth in which PV operates is lower than OLTC. Due to this Q-V droop will regulate voltage at much lower level. It was observed that all the voltages were within the limits however the the magnitude was higher as compared to OLTC operation. The loading of PV also increases with increase in reactive power absorption. When the OLTC and Q-V droop are operated simultaneously without any coordination, the tap change requirement increases. With proper coordinated control as proposed, the tap change is minimized and the voltage magnitude are also under permissible range.

6.2 Future Work

This section enlists several relevant ideas which can be implemented in future work. In this thesis, quasi-dynamic analysis has been analyzed. Hence an investigation of dynamic behaviour can be implemented. Furthermore, detailed model of PV can be implemented

rather than a static generator. Impact of other type of autonomous control and its performance evaluation in presence of OLTC can also be investigated. Additional regulating units such as shunt capacitors, energy storage devicss can aslo be included

Bibliography

[1] *Global Market Outlook 2019-2023 - SolarPower Europe*. http://www.solarpowereurope.org/global-market-outlook-2019-2023/. (Accessed on 07/22/2019).

[2] *METIS Study-Effect of high shares of renewables on power systems*. https://www.irena.org/-/media/Files/IRENA/Agency/Publication/2018/Feb/IRENA_REmap_EU_2018.pdf. (Accessed on 07/22/2019).

[3] *Model Analysis of Flexibility of the Danish Power System*. https://ens.dk/sites/ens.dk/files/Globalcooperation/Publications_reports_papers/model_analysis_of_flexibility_of_the_danish_power_system.2018.05.15.pdf. (Accessed on 07/22/2019).

[4] *Effect of high shares of renewables on power systems - Publications Office of the EU*. https://publications.europa.eu/en/publication-detail/-/publication/01c456f4-7144-11e9-9f05-01aa75ed71a1/language-en/format-PDF/source-96288175. (Accessed on 07/22/2019).

[5] M Karimi, H Mokhlis, K Naidu, et al. "Photovoltaic penetration issues and impacts in distribution network–A review". In: *Renewable and Sustainable Energy Reviews* 53 (2016), pp. 594–605.

[6] Ferry A Viawan, Ambra Sannino, and Jaap Daalder. "Voltage control with on-load tap changers in medium voltage feeders in presence of distributed generation". In: *Electric power systems research* 77.10 (2007), pp. 1314–1322.

[7] Bianca Barth Zuzana Musilova Paolo Michele Sonvilla Carlos Mateo Riccardo Lama et al. *European Advisory Paper*. https://ec.europa.eu/energy/intelligent/projects/sites/iee-projects/files/projects/documents/pv_grid_european_advisory_paper_july_2014_annex_ii.pdf. Apr. 2018.

[8] Xiaohu Liu, Andreas Aichhorn, Liming Liu, et al. "Coordinated control of distributed energy storage system with tap changer transformers for voltage rise mitigation under high photovoltaic penetration". In: *IEEE Transactions on Smart Grid* 3.2 (2012), pp. 897–906.

[9] Ellen Liu and Jovan Bebic. *Distribution system voltage performance analysis for high-penetration photovoltaics*. Tech. rep. National Renewable Energy Lab.(NREL), Golden, CO (United States), 2008.

[10] Satoru Akagi, Shinya Yoshizawa, Jun Yoshinaga, et al. "Capacity determination of a battery energy storage system based on the control performance of load leveling and voltage control". In: *Journal of International Council on Electrical Engineering* 6.1 (2016), pp. 94–101.

[11] Kashem M Muttaqi, An DT Le, Michael Negnevitsky, et al. "A coordinated voltage control approach for coordination of OLTC, voltage regulator, and DG to regulate voltage in a distribution feeder". In: *IEEE Transactions on Industry Applications* 51.2 (2015), pp. 1239–1248.

[12] Stefano Barsali et al. *Benchmark systems for network integration of renewable and distributed energy resources*. 2014.

[13] K Prakash, A Lallu, FR Islam, et al. "Review of power system distribution network architecture". In: *2016 3rd Asia-Pacific World Congress on Computer Science and Engineering (APWC on CSE)*. IEEE. 2016, pp. 124–130.

[14] DigSilent. *PowerFactory User Manual*. `https://www.digsilent.de/en/`. (Accessed on 09/01/2019). 2019.

[15] Rene Prenc, Davor Škrlec, and Vitomir Komen. "A novel load flow algorithm for radial distribution networks with dispersed generation". In: *Technical Gazette* 20.6 (2013), pp. 969–977.

[16] Dusko Nedic. "Tap adjustment in AC load flow". In: *UMIST*. 2002.

[17] CL Wadhwa. *Electrical power systems*. New Age International, 2006.

[18] Turan Gonen. *Electric power distribution engineering*. CRC press, 2015.

[19] "IEEE Recommended Practice for Electric Power Distribution for Industrial Plants". In: *IEEE Std 141-1993* (1994), pp. 1–768. DOI: `10.1109/IEEESTD.1994.121642`.

[20] Ferry Viawan. *Voltage control and voltage stability of power distribution systems in the presence of distributed generation*. Chalmers University of Technology, 2008.

[21] Dr. Dieter Dohnal. *On-Load Tap-Changers For Power Transformers*. `https://www.reinhausen.com/de/XparoDownload.ashx?raid=58092`. (Accessed on 08/08/2019).

[22] J-H Choi and J-C Kim. "The online voltage control of ULTC transformer for distribution voltage regulation". In: *International Journal of Electrical Power & Energy Systems* 23.2 (2001), pp. 91–98.

[23] Math HJ Bollen and Fainan Hassan. *Integration of distributed generation in the power system*. Vol. 80. John wiley & sons, 2011.

[24] Bo Zhao, Xuesong Zhang, and Jian Chen. "Integrated microgrid laboratory system". In: *IEEE Transactions on power systems* 27.4 (2012), pp. 2175–2185.

[25] Joan Rocabert, Alvaro Luna, Frede Blaabjerg, et al. "Control of power converters in AC microgrids". In: *IEEE transactions on power electronics* 27.11 (2012), pp. 4734–4749.

[26] A Tuladhar, H Jin, T Unger, et al. "Parallel operation of single phase inverter modules with no control interconnections". In: *Proceedings of APEC 97-Applied Power Electronics Conference*. Vol. 1. IEEE. 1997, pp. 94–100.

[27] Hua Han, Xiaochao Hou, Jian Yang, et al. "Review of power sharing control strategies for islanding operation of AC microgrids". In: *IEEE Transactions on Smart Grid* 7.1 (2015), pp. 200–215.

[28] N Karthikeyan, Basanta Raj Pokhrel, Jayakrishnan R Pillai, et al. "Coordinated voltage control of distributed PV inverters for voltage regulation in low voltage distribution networks". In: *2017 IEEE PES Innovative Smart Grid Technologies Conference Europe (ISGT-Europe)*. IEEE. 2017, pp. 1–6.

[29] Askari Mohammad Bagher, Mirzaei Mahmoud Abadi Vahid, and Mirhabibi Mohsen. "Types of solar cells and application". In: *American Journal of optics and Photonics* 3.5 (2015), pp. 94–113.

[30] D Energinet. "Technical regulation 3.2. 2 for PV power plants with a power output above 11 kW". In: *Tech. Rep.* (2015).

[31] Erhan Demirok, Pablo Casado Gonzalez, Kenn HB Frederiksen, et al. "Local reactive power control methods for overvoltage prevention of distributed solar inverters in low-voltage grids". In: *IEEE Journal of Photovoltaics* 1.2 (2011), pp. 174–182.

[32] John J Grainger, William D Stevenson, William D Stevenson, et al. *Power system analysis*. 2003.

[33] HM Ayres, W Freitas, MC De Almeida, et al. "Method for determining the maximum allowable penetration level of distributed generation without steady-state voltage violations". In: *IET generation, transmission & distribution* 4.4 (2010).

[34] Fracisco M González-Longatt et al. "Impact of distributed generation over power losses on distribution system". In: *9th International conference on electrical power quality and utilization*. 2007.

[35] Deependra Singh, Devender Singh, and KS Verma. "Multiobjective optimization for DG planning with load models". In: *IEEE transactions on power systems* 24.1 (2009), pp. 427–436.

[36] Alexandra Von Meier. “Integration of renewable generation in California: Coordination challenges in time and space”. In: *11th International Conference on Electrical Power Quality and Utilisation*. IEEE. 2011, pp. 1–6.

[37] Dispersed Generation Photovoltaics and Energy Storage. “IEEE Standard for Interconnection and Interoperability of Distributed Energy Resources with Associated Electric Power Systems Interfaces”. In: ().